Article
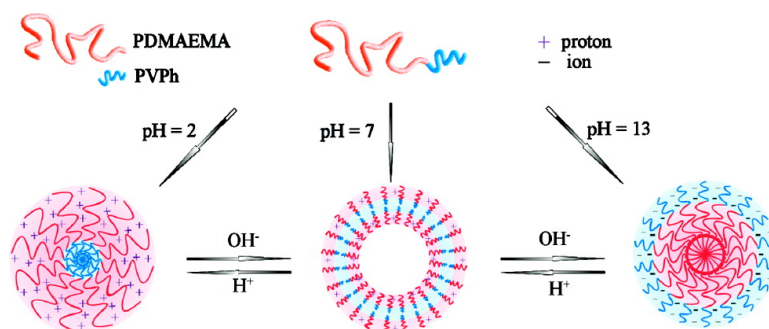
Syntheses, Specific Interactions, and pH-Sensitive Micellization Behavior of Poly[vinylphenol-*b*-2-(dimethylamino)ethyl methacrylate] Diblock Copolymers

Shih-Chien Chen, Shiao-Wei Kuo, Chun-Syong Liao, and Feng-Chih Chang

More About This Article

Additional resources and features associated with this article are available within the HTML version:

- Supporting Information
- Access to high resolution figures
- Links to articles and content related to this article
- Copyright permission to reproduce figures and/or text from this article

View the Full Text HTML

Syntheses, Specific Interactions, and pH-Sensitive Micellization Behavior of Poly[vinylphenol-*b*-2-(dimethylamino)ethyl methacrylate] Diblock Copolymers

Shih-Chien Chen,[†] Shiao-Wei Kuo,*,‡ Chun-Syong Liao,[†] and Feng-Chih Chang*,†

Institute of Applied Chemistry, National Chiao Tung University, Hsinchu 300, Taiwan, and Department of Materials and Optoelectronic Science, Center for Nanoscience and Nanotechnology, National Sun Yat-Sen University, Kaohsiung 804, Taiwan

ABSTRACT: We have used anionic polymerization to prepare a series of poly[vinylphenol-*b*-2-(dimethylamino)ethyl methacrylate] (PVPh-*b*-PDMAEMA) block copolymers. These block copolymers are miscible, with strong specific interactions occurring between the OH groups of the PVPh segments and the tertiary ammonium groups of the PDMAEMA segments. These PVPh-*b*-PDMAEMA diblock copolymers exhibit higher glass transition temperatures than do the corresponding PVPh/partially protonated PDMAEMA blends obtained from DMSO solution, which we suspect exist in the form of separate coils. The blocks of the PVPh-*b*-PDMAEMA diblock copolymers interact strongly, resulting in polymer complex aggregation similar to the behavior of PVPh/partially protonated PDMAEMA blend complexes obtained from methanol solution. The spin−lattice relaxation times in the rotating frame, determined through solid state NMR spectroscopic analysis, provided clear evidence that the polymer complex aggregates formed from the diblock copolymers have shorter values of $T_{1\rho}^{\mathrm{H}}$ than do the corresponding separated coils in the miscible blends. In addition, these PVPh-*b*-PDMAEMA diblock copolymers exhibit a novel type of pH sensitivity: at low pH, compact spherical micelles are formed possessing PDMAEMA coronas and PVPh cores; at medium pH, vesicles are observed, consisting of partially protonated hydrophilic PDMAEMA shells and hydrophobic PVPh cores; at high pH, the spherical micelles that formed comprised ionized PVPh coronas and deprotonated hydrated-PDMAEMA cores, i.e., phase inversion of the micelles formed at pH 2.

Introduction

A vast majority of the studies aimed at enhancing the miscibility of polymer blends have involved incorporating local centers capable of participating in strong noncovalent interactions (e.g., ion−ion, ion−dipole, and hydrogen-bonding interactions) into the blend components.[1−3] It is well-known that the strength and extent of hydrogen bonding in copolymers or polymer blends depend on the respective affinities between the hydrogen bond donors and acceptors.[4−6] Because poly(vinylphenol) (PVPh) possesses strong proton-donor groups, it is miscible with proton-acceptor polymers such as poly(methacrylate), polyether, and polyester.[7−12] Poly[(dimethylamino)ethyl methacrylate] (PDMAMEA) possesses three possible proton-accepting sites: the C=O oxygen, ether oxygen, and nitrogen atoms. Goh et al. studied the miscibility and thermal behavior of PVPh/PDMAEMA blends in low-polarity solvents (e.g., methanol, ethanol, and MEK).[13] The nature of the solvent plays an important role affecting the formation of polymer complexes.[14] For example, PVPh/poly(*N*,*N*-dimethylacrylamide) (PDMA) blends form a complex precipitate in dioxane but do not precipitate from DMF. Because solvent molecules can also participate in hydrogen-bonding interactions, they compete with PDMA for coordination to the OH groups of PVPh. Consequently, when the polymer−polymer interactions are sufficiently strong to overcome the polymer−solvent interactions, the two polymer chains can coprecipitate in the form of highly associated materials (complexes). If the solvent interacts so strongly with the polymers that it prevents precipitation, the resulting materials obtained upon evaporation of the solvent are considered to be merely blends. In general, a single glass transition temperature (T_g) is obtained for both miscible blends and complexes, indicating that they are single-phase materials. Nevertheless, the values of T_g of complexes are usually higher than those of miscible blends having similar compositions because of the more compact nature of the complexes.[15−19] In a previous study, we observed the interesting result that PVPh-*b*-poly(4-vinylpyridine) (P4VP) diblock copolymers possess higher values of T_g relative to those of their corresponding PVPh/P4VP blends. These diblock copolymers may form inter- and intrapolymer complex aggregates similar to the PVPh/P4VP complexes obtained from methanol solution.[20] Although the polymer chain behavior of these diblock copolymers is similar to that of its corresponding blend complexes, it is not clear whether the same conclusion is applicable to all diblock copolymers experiencing strong interactions.

Multiple-stimulus-responsive copolymers that are soluble in water are attracting increasing attention because of their diverse self-assembly behavior in response to such stimuli as pH, temperature, and ionic strength.[21−32] These copolymers can form two or more types of aggregates, including inverted structures, upon judicious adjustment of the environmental conditions. Therefore, depending upon the response to an applied stimulus, a number of applications can be contemplated for the same precursor copolymer, e.g., cosmetics, detergents, encapsulation, drug delivery, and enhanced recognition of a predetermined target. The first findings in this field, dealing with poly[2-(diethylamino)ethyl methacrylate-*b*-2-(*N*-morpholino)ethyl methacrylate] (PDEA-*b*-PMEMA), were reported by Armes in 1998.[21,22] The diblock copolymer was dissolved in aqueous media at pH 4, and then PDEA−core micelles were formed merely by adjusting the solution pH. The formation of inverted PMEMA−core micelles occurred upon the addition of an electrolyte through selective "salting out" of the PMEMA block.

* To whom correspondence should be addressed. For F.-C.C.: e-mail, changfc@mail.nctu.edu.tw; phone, 886-3-5131512, fax, 886-3-5131512. For S.-W.K.: e-mail, kuosw@faculty.nsysu.edu.tw; fax, 886-7-5254099.
† National Chiao Tung University.
‡ National Sun Yat-Sen University.

Scheme 1. Synthesis of Poly[vinylphenol-*b*-2-(dimethylamino)ethyl methacrylate] Diblock Copolymers Using Anionic Polymerization
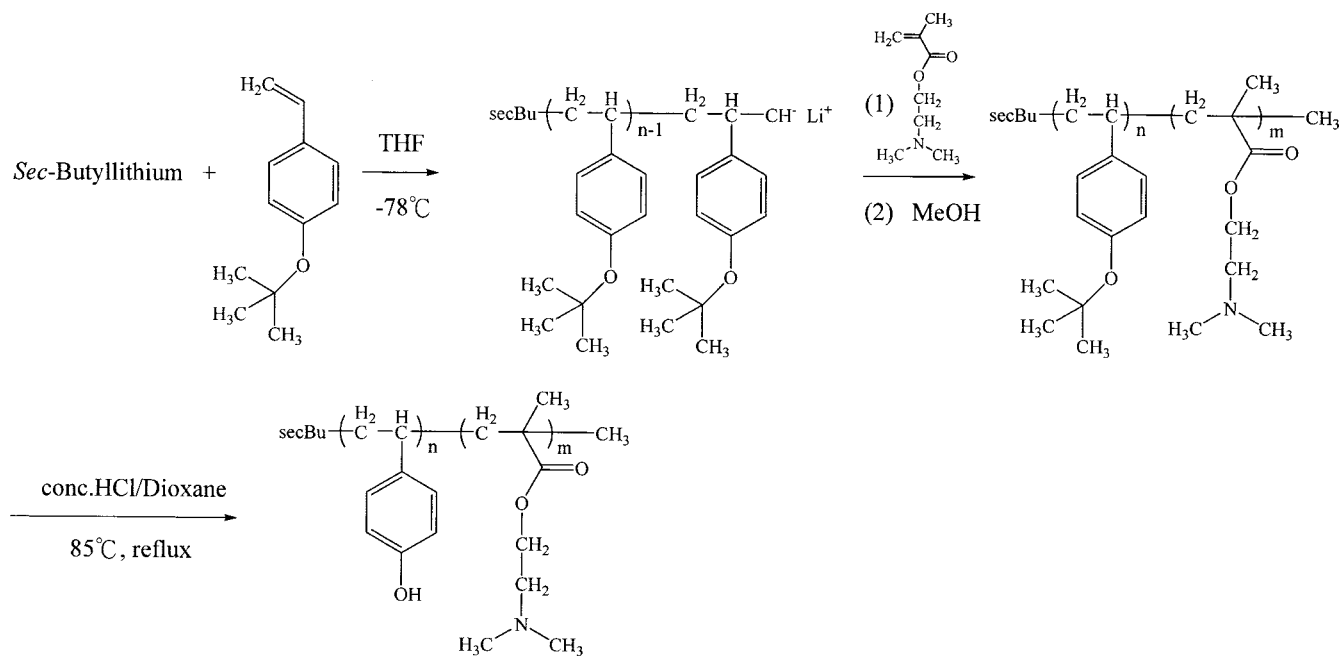
The second known example was that of poly[propylene oxide-*b*-2-(diethylamino)ethyl methacrylate] (PPO-*b*-PDEA), which possesses a thermally sensitive PPO block and a pH-sensitive PDEA block.[23] This diblock copolymer dissolved in cold water at pH 6.5 but formed PPO–core micelles upon increasing the temperature; the PDEA–core micelles were obtained by increasing the pH to 8.5 at 5 °C. Several other sensitive copolymers have been investigated since then, including the block copolymers poly[succinyl ethyl methacrylate-*b*-2-(diethylamino)ethyl methacrylate] (PSEMA-*b*-PDEAEMA),[24] poly[4-vinylbenzoic acid-*b*-2-(*N*-morpholino)ethyl methacrylate] (PVBA-*b*-PMEMA),[25] and poly(hydroxystyrene-*b*-methacrylic acid) (PSOH-*b*-PMAA).[26]

In this paper, we report the preparation of a series of novel pH-sensitive PVPh-*b*-PDMAEMA diblock copolymers by combining protected group chemistry with anionic polymerization. Using ^{1}H NMR spectroscopy, DSC, FTIR spectroscopy, 2D correlation-IR spectroscopy, and ^{13}C solid state NMR spectroscopy, we characterized the chemical structures, glass transition behavior, specific interactions, and polymer chain behavior of these diblock copolymers. Additionally, we investigated the pH-sensitive reversible micellization behavior of these PVPh-*b*-PDMAEMA diblock copolymers using ^{1}H NMR spectroscopy and TEM analyses.

Experimental Section

Materials. 4-*tert*-Butoxystyrene (*t*BOS, Aldrich, 99%) and 2-(dimethylamino)ethyl methacrylate (DMAEMA, Aldrich, 99%) were distilled from finely ground CaH$_2$ prior to use. Tetrahydrofuran (THF), the polymerization solvent for anionic polymerization, was purified through distillation under argon from a red solution of diphenylhexyllithium [produced through the reaction of 1,1-diphenylethylene and *n*-butyllithium (*n*-BuLi)]. *sec*-BuLi (Acros, 1.3 M in cyclohexane) was used as the initiator for anionic polymerization.

Poly[vinylphenol-*b*-2-(dimethylamino)ethyl methacrylate] Diblock Copolymer. Poly[4-*tert*-butoxystyrene-*b*-2-(dimethylamino)ethyl methacrylate] (P*t*BOS-*b*-PDMAEMA) diblock copolymer was synthesized through sequential living anionic polymerization of *t*BOS and DMAEMA in THF, using *sec*-BuLi as initiator (Scheme 1). Lithium chloride (LiCl) was added to prevent side

reactions.[33–37] Polymerizations were performed in THF at −78 °C under an inert atmosphere. The *t*BOS monomer was polymerized first for 2 h; an aliquot of the poly(*t*BOS) was isolated for analysis after termination with degassed methanol. DMAEMA was then introduced into the reactor; the reaction was terminated after 2 h through the addition of degassed methanol.

The P*t*BOS-*b*-PDMAEMA copolymer was converted into PVPh-*b*-PDMAEMA through hydrolysis. The P*t*BOS-*b*-PDMAEMA diblock copolymer product was dissolved in dioxane, and then a 10-fold excess of 37 wt % hydrochloric acid was added to the solution. The hydrolysis was continued for 2 days at 85 °C under an atmosphere of argon, and then the product was neutralized to pH 8 with 10 wt % aqueous NaOH. The resulting solution was purified for 2 weeks through dialysis against regularly distilled water; the product was then precipitated in cold ethyl ether. Before drying under vacuum, the final copolymer was subjected to two dissolve (DMF)/precipitate (ethyl ether) cycles.

Using a living anionic polymerization procedure similar to the one described above, the homopolymer of PVPh was synthesized to compare its thermal properties with those of the copolymers. In additional, the homopolymer of PDMAEMA was synthesized through atom transfer radical polymerization using ethyl α-bromoisobutyrate as initiator; the degree of protonation was adjusted to ca. 15% using HCl (partially protonated PDMAEMA).

Blend Preparation. Blends of PVPh/partially protonated PDMAEMA (15% protonation) were prepared through solution-casting. Separate DMSO solutions of pure PVPh and pure partially protonated PDMAEMA were stirred together in various molar ratios. The resulting polymer mixtures were stirred for 1 day and then cast onto Teflon dishes. The samples were then left to evaporate slowly at 100 °C for 1 day. The blend films were then dried for 1 week under vacuum at 100 °C.

Characterization. Molecular weights and molecular weight distributions were determined through gel permeation chromatography (GPC) using a Waters 510 HPLC equipped with a 410 differential refractometer, a RI detector, a UV detector, and three Ultrastyragel columns (100, 500, and 10^3 Å) connected in series; THF was the eluent; the flow rate was 0.6 mL/min at 35 °C. The molecular weight calibration curve was obtained using polystyrene standards. ^{1}H and ^{13}C NMR spectra were obtained using an INOVA 500 instrument; CDCl$_3$ and dimethyl-d_6 sulfoxide were used as the solvents. The molecular weights and P*t*BOS/PDMAEMA ratios of

Scheme 2. Schematic Representation of the Types of Interactions that Exist between PVPh-*b*-PDMAEMA Diblock Copolymer Units
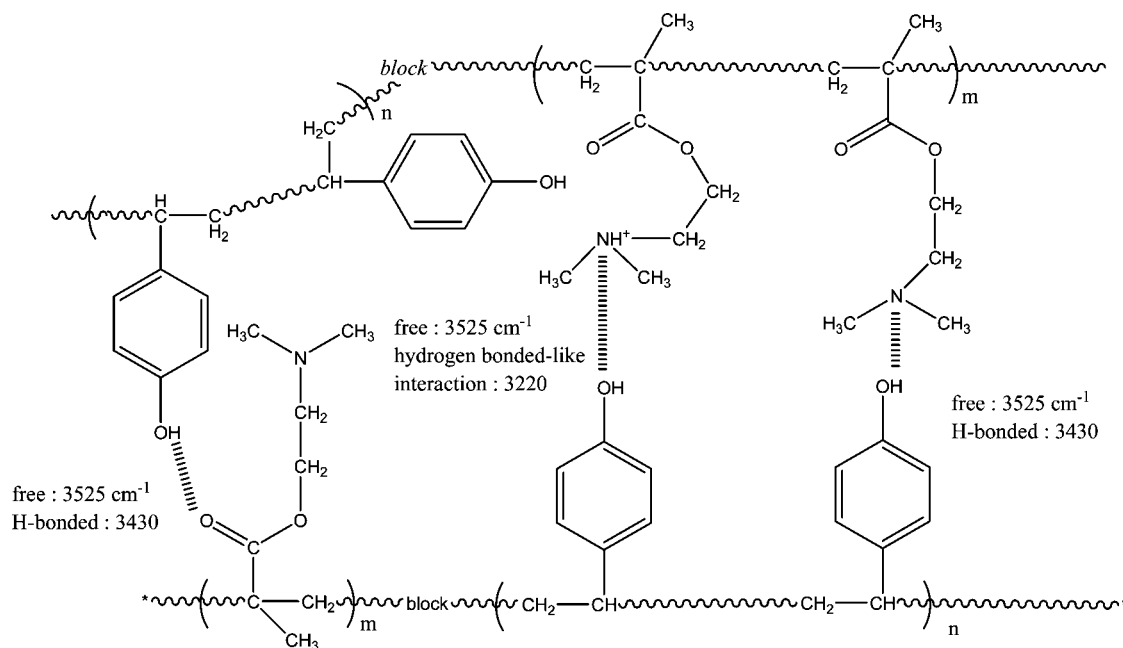
the various copolymers were evaluated from ¹H NMR spectra and compared with the corresponding values obtained from GPC analysis. All infrared (IR) spectra were recorded under nitrogen using a Nicolet Avatar 320 FTIR spectrometer; 32 scans were collected at resolution of 1 cm⁻¹. Each sample was dissolved in DMSO and then cast directly onto a KBr pellet. All of the vacuum-dried films were sufficiently thin within the absorbance range such that the Beer–Lambert law was obeyed. 2D correlation analysis was performed using the 2D Shige software programmed by Shigeaki Morita (Kwansei-Gakuin University, Japan). All of the spectra applied to the 2D-IR correlation analyses were normalized; the negative intensities of the auto- or cross-peaks in 2D-IR correlation spectra were indicated by blue regions; positive intensities were indicated by red regions. Thermal analyses were performed using a DuPont 910 controller operated at a scan rate of 20 °C/min over the temperature range from −60 to +250 °C under a nitrogen atmosphere. The sample (ca. 5–10 mg) was weighted and sealed in an aluminum pan, quickly quenched to −60 °C from the first scan, and then rescanned between −60 and +250 °C at a scan rate of 20 °C/min. The glass transition temperature was obtained as the inflection point of the heat capacity jump. High-resolution solid state ¹³C NMR spectra were recorded at 25 °C using a Bruker DSX-400 spectrometer operating at resonance frequencies of 399.53 and 100.47 MHz for ¹H and ¹³C, respectively. The ¹³C CP/MAS spectra were measured using a 3.9 μs 90° pulse, a 3 s pulse delay time, a 30 ms acquisition time, and 2048 scans. All NMR spectra were recorded at 300 K using broadband proton decoupling and a normal cross-polarization pulse sequence. A magic-angle sample spinning (MAS) rate of 5.4 kHz was used to avoid absorption overlapping. The proton spin–lattice relaxation time in the rotating frame ($T_{1\rho}^{H}$) was determined indirectly via carbon observation using a 90°–τ–spin lock pulse sequence prior to cross-polarization. The data acquisition was performed via ¹H decoupling with delay times ranging from 0.1 to 20 ms and a contact time of 1.0 ms. For transmission electron microscopy (TEM) studies, a drop of the micelle solution was sprayed onto a Cu TEM grid covered with a Formvar support film that had been precoated with a thin film of carbon. After 1 min, the excess of the solution was blotted away using a strip of filter paper. All samples were left to dry at room temperature for 1 day prior to observation. After drying, the samples were stained with RuO₄ and viewed under a Hitachi H-7500 TEM instrument operated with an accelerating voltage of 100 kV.

Results and Discussion

Syntheses of Poly[vinylphenol-*block*-2-(dimethylamino)-ethyl methacrylate] Diblock Copolymers. The PVPh-*b*-PDMAEMA diblock copolymers were prepared through anionic living polymerization of P*t*BOS-*b*-PDMEMA and subsequent hydrolytic deprotection. The hydrolysis of the P*t*BOS-*b*-PDMAEMA copolymers, performed at 85 °C in dioxane in the presence of concentrated HCl, gave the PVPh-*b*-PDMAEMA diblock copolymers quantitatively (Scheme 1). The molecular weights and polydispersities of the pure P*t*BOS and P*t*BOS-*b*-PDMAEMA diblock copolymers were analyzed using GPC.

¹H and ¹³C NMR spectra were recorded from P*t*BOS-*b*-PDMAEMA and PVPh-*b*-PDMAEMA to confirm their chemical compositions and structures. Figure 1 displays typical ¹H NMR spectra of the diblock copolymers recorded before and after deprotection, together with assignments of their characteristic peaks. The signal at 1.29 ppm, corresponding to the *tert*-butyl groups of the P*t*BOS-*b*-PDMAEMA copolymer (in CDCl₃), disappeared in the spectrum of the hydrolyzed block copolymer,
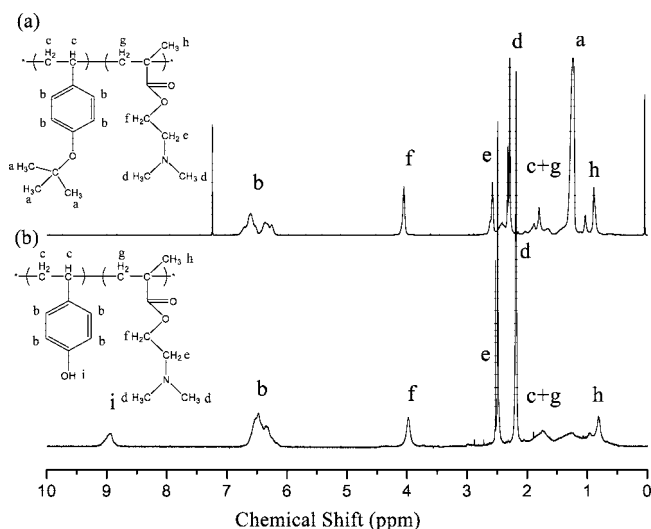
Figure 1. ¹H NMR spectra: (a) before hydrolysis, P*t*BOS-*b*-PDMAEMA; (b) after hydrolysis, PVPh-*b*-PDMAEMA.
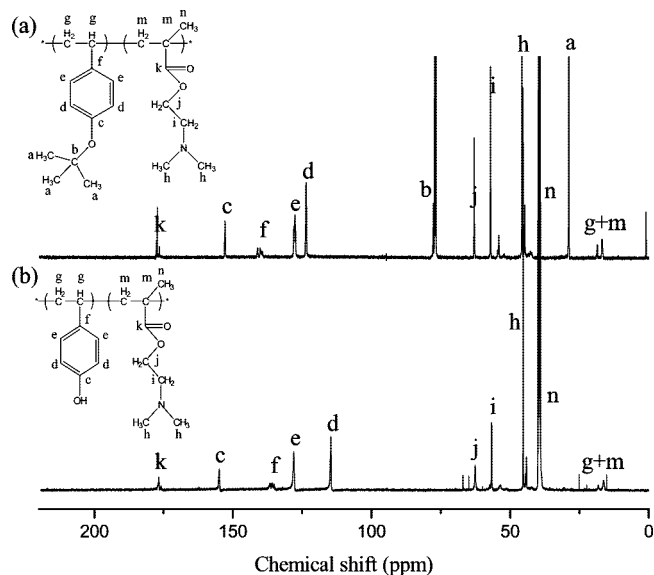
Figure 2. ^{13}C NMR spectra: (a) before hydrolysis, P*t*BOS-*b*-PD-MAEMA; (b) after hydrolysis, PVPh-*b*-PDMAEMA.

and only the signals of the polymer backbone protons appear in the region 1−2 ppm. In addition, a peak (8.9 ppm), corresponding to the protons of the OH groups, appears after hydrolysis. Figure 2a reveals that the signal of the quaternary carbon atom of the *tert*-butyl group in the P*t*BOS segment appeared at 78.0 ppm.[38] After hydrolysis, this signal disappeared (Figure 2b), indicating that the hydrolysis reaction was complete. The FTIR spectrum (Figure S1) of the block copolymer after hydrolysis still clearly exhibits the C=O stretching vibration band of the PDMEMA segment in the region from 1690 to 1750 cm^{-1}. The broad peak at 3300 cm^{-1} in Figure S1c indicates the presence of OH groups after deprotection. The compositions of the PVPh-*b*-PDMAEMA block copolymers were essentially identical to those of the corresponding P*t*BOS-*b*-PDMAEMA block copolymers, as determined from the relative intensities of the peaks of the aromatic rings and the ethyl protons, located at 6.1−6.9 and 4.1−4.2 ppm, respectively. Table 1 lists the molecular parameters of the polymers and summarizes the characterization data for each PVPh-*b*-PDMAEMA copolymer.

FTIR Spectroscopic Analyses. FTIR spectroscopy has been successfully applied to the analysis of numerous diblock copolymers and blends featuring intermolecular hydrogen-bonding interactions. The OH stretching region in the IR spectra of PVPh-*b*-PDMAEMA diblock copolymers is sensitive to the degree and type of hydrogen bonding. Figure 3 displays the OH stretching region (2700−4000 cm^{-1}) of the FTIR spectra of the pure PVPh and various PVPh-*b*-PDMAEMA diblock copolymers cast from DMSO solution at room temperature. The spectrum of pure PVPh reveals two unresolved bands in the OH stretching region, corresponding to the free OH groups at 3525 cm^{-1} and a broad band centered at 3350 cm^{-1} arising from the absorption of hydrogen-bonded OH groups (self-association).[20] Figure 3 indicates that the intensity of the signal of the free OH groups decreased gradually upon increasing the PDMAEMA content in the diblock copolymer; i.e., a greater fraction of OH groups interacted with PDMAEMA upon increasing the PDMAEM content. In the meantime, the intensity of the OH stretching band shifted to lower wavenumber upon increasing the DMAEMA content, indicating that a new distribution of the OH stretching region was formed from competition between the multiply hydrogen-bonded OH groups within the pure PVPh and the specific interactions between PVPh and PDMAEMA. Surprisingly, the trend is different from that observed by Goh et al.,[7] who found that the signal for

OH−OH hydrogen bonding (3350 cm^{-1}) shifted to higher wavenumber (3430 cm^{-1}) upon increasing the PDMAEMA content in the PVPh/PDMAEMA blend system because of the formation of hydrogen bonds between the OH groups of PVPh and the C=O oxygen atoms and N atoms of PDMAEMA.

We suspected that the differences observed between the FTIR spectra of the block copolymer system and the blend system may have arisen from different types of noncovalent interactions in these systems. According to the procedure employed for the synthesis of the block copolymer, tertiary ammonium groups are formed from the hydrolysis reaction. Although our block copolymer was neutralized with 10 wt % NaOH solution to pH 8 after hydrolysis, a small fraction of tertiary ammonium groups would still be present in the block copolymer. Therefore, we speculated that the difference in the IR spectra resulted from the formation of stronger specific interactions between the OH groups of PVPh and the tertiary ammonium groups of PD-MAEMA. Thus, we prepared a model blend corresponding to our block copolymer, i.e., a PVPh/fully protonated PDMAEMA blend. Figure S2 displays the OH stretching region of the FTIR spectra of the pure PVPh and the PVPh/fully protonated PDMAEMA blend. The PVPh/fully protonated PDMAEMA blend and our block copolymer system exhibit a similar trend: the broad hydrogen-bonded OH band shifted to lower wavenumber for the PVPh/fully protonated PDMAEMA blend, thereby confirming the presence of a specific interaction between the OH groups of PVPh and the tertiary ammonium groups of PDMAEMA. According to Pullman's study of the interactions between the tetramethylammonium (TMA) ion and phenol, the phenol leans toward one hydrogen atom of TMA while the O−H bond rotates out of the molecular plane to orient the oxygen atom's lone pair optimally (O···H distance: 2.35 Å; OH rotation: 32°); the formation of the "hydrogen-bond-like" interaction clearly gives rise to the increment in stability observed with respect to benzene−TMA.[39] Our spectroscopic investigation confirmed that the specific (hydrogen-bond-like) interaction was formed via the oxygen atom's lone pair of electrons interacting with the charge of the tertiary ammonium groups. It is reasonable to assign the band at 3220 cm^{-1} to the signal of OH groups of PVPh hydrogen bonding to the tertiary ammonium groups of PDMAEMA. In addition, we used titration analysis to determine that the degree of protonation of the diblock copolymers was ca. 15%.

Taking into account the effect of the composition, the tertiary ammonium groups of PDMAEMA compete with self-associated OH groups, the C=O oxygen atoms, and the nitrogen atoms of PDMAEMA for hydrogen-bonding opportunities, causing the shift of the signal for the OH band toward lower wavenumbers gradually upon decreasing the vinylphenol content. Coleman and co-workers used the frequency difference (Δv) between the hydrogen-bonded and free OH absorptions to roughly estimate the average hydrogen bond strength.[40] In this respect, on the basis of the reference of the free OH stretching band at 3525 cm^{-1}, the frequency differences resulting from OH···C=O (Δv = 95 cm^{-1}), OH···N (Δv = 95 cm^{-1}), and OH···OH (Δv = 175 cm^{-1}) interactions are all weaker than the OH···tertiary ammonium interactions (Δv = 305 cm^{-1}). In this situation, only the latter type of interaction is predominant and, thus, the OH stretching band is relatively narrow.

Next, we turned our attention to compare the chain behavior of the blend systems with that of the block copolymer system. To compare the chain behavior, we blended PVPh with partially protonated PDMAEMA. Figure S3 displays the OH stretching region of the FTIR spectra of the pure PVPh and various PVPh/partially protonated PDMAEMA blends. The spectra are similar to those of the block copolymer system: the peak for the broad OH stretching band shifts to lower wavenumber upon increasing

Table 1. Molecular Characterization of Poly[vinylphenol-*b*-2-(dimethylamino)ethyl methacrylate] Diblock Copolymers Prepared Using Anionic Polymerization

precursor copolymer	copolymer	$M_{n,PtBOS}{}^{a}$	total $M_n{}^{a}$	PVPh (mol %)^{b}	$M_w/M_n{}^{a}$	T_g (°C)
P*t*BOS	PVPh	14 600	10 000	100	1.05	172
P*t*BOS$_{16}$-*b*-PDMAEMA$_{84}$	PVPh$_{16}$-*b*-PDMAEMA$_{84}$	2 900	17 300	14	1.11	113
P*t*BOS$_{32}$-*b*-PDMAEMA$_{68}$	PVPh$_{32}$-*b*-PDMAEMA$_{68}$	5 280	13 650	32	1.11	136
P*t*BOS$_{55}$-*b*-PDMAEMA$_{45}$	PVPh$_{55}$-*b*-PDMAEMA$_{45}$	11 100	15 400	55	1.15	184
P*t*BOS$_{70}$-*b*-PDMAEMA$_{30}$	PVPh$_{70}$-*b*-PDMAEMA$_{30}$	16 100	16 300	70	1.10	177
	PDMAEMA		14 130	0	1.10	14

^{a} Polydispersity index and molecular weight, measured by GPC, of the whole diblock copolymer in the form of P*t*BOS-*b*-P4VP. ^{b} Obtained from ^{1}H NMR measurement.
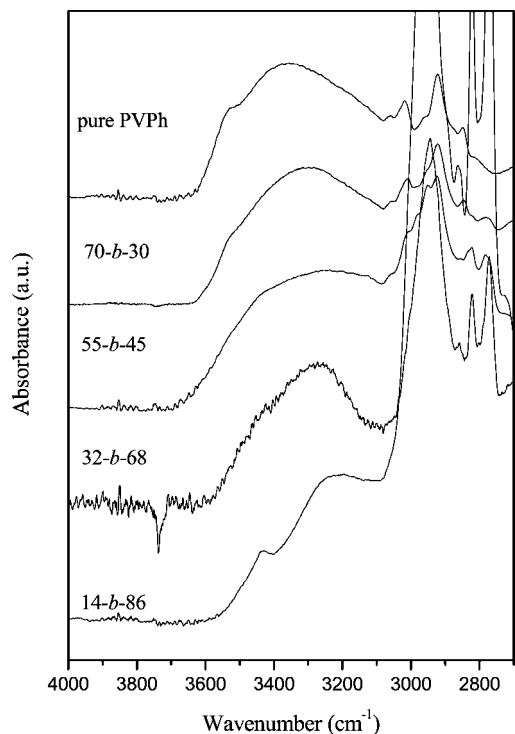
Figure 3. FTIR spectra (room temperature, OH stretching region) of PVPh-*b*-PDMAEMA diblock copolymers cast from DMSO solutions.

the content of partially protonated PDMAEMA because of the specific interactions between the OH groups of PVPh and the tertiary ammonium groups of PDMAEMA. Thus, specific interactions are indeed formed between the OH groups of PVPh and the tertiary ammonium groups of PDMAEMA.

Figure S4 presents the scale-expanded FTIR spectra (C=O stretching range; 1660−1800 cm^{-1}) of pure PVPh, pure PDMAEMA, the PVPh-*b*-PDMAEMA block copolymers, and their blends. The peaks at 1730 and 1705 cm^{-1} correspond to the free and hydrogen-bonded C=O groups, respectively. As expected, a higher number of hydrogen-bonded C=O groups result at a higher content of vinylphenol units. To obtain the fraction of hydrogen-bonded C=O group, it is necessary to know the absorptivity ratio for the contributions of hydrogen-bonded and free C=O groups; we employed the value of α_{HB}/α_F of 1.5 that had previously been calculated by Moskala et al.[41] Table 2 summarizes the fraction of hydrogen-bonded C=O groups, as determined through curve fitting of the data from the copolymers and binary blends. The fraction of hydrogen-bonded C=O groups increased upon increasing the PVPh content for both the PVPh-*b*-PDMAEMA and PVPh/partially protonated PD-MAEMA blend systems. Moreover, the fraction of hydrogen-bonded C=O groups of the copolymers was always higher than that of the blend system at similar PVPh contents. This observation can be explained in terms to the difference in the degrees of rotational freedom of the polymer blend and block

copolymer.[42] The polymer chain architecture of a homopolymer blend is significantly different from that of a copolymer because of intramolecular screening.[43−47] The PVPh segment in a copolymer system has more contacts with PDMAEMA segments than it does in blend systems because of both chain connectivity and intramolecular screening effects. Intramolecular screening results from an increase in the number of same-chain contacts due to polymer chains bending back upon themselves. This "screening" process reduces the number of intermolecular hydrogen bonds formed in a polymer blend. Thus, the interassociation hydrogen-bonding density of a copolymer system is relatively higher than that of a corresponding blend system. As a result, the density of hydrogen-bonded C=O groups in the PVPh/partially protonated PDMAEMA blend was relatively lower than that in the corresponding PVPh-*b*-PDMAEMA copolymer having the same composition.

2D-IR Correlation Analyses. To further understand the chain behavior and the order of the interaction for block copolymer and its blend, we recorded 2D-IR correlation spectra for the PVPh-*b*-PDMAEMA copolymer and the PVPh/partially protonated PDMAEMA blends. Throughout this paper, the blue and red regions of the 2D-IR correlation counter maps indicate negative and positive correlation intensities, respectively. We obtained two types of spectra: 2D synchronous and asynchronous spectra. The intensity of a signal in a synchronous 2D-IR correlation spectrum $\Phi(v_1,v_2)$ represents the simultaneous or coincidental change of the spectral intensity variations measured at v_1 and v_2; the intensity of a signal in an asynchronous spectrum $\Psi(v_1,v_2)$ represents sequential or successive changes of spectral intensities observed at v_1 and v_2. The sign of a synchronous cross-peak [$\Phi(v_1,v_2)$] becomes positive if the intensity variations of the two peaks v_1 and v_2 follow the same trend (both increase or both decrease) under the environmental perturbation. On the other hand, the sign of an asynchronous cross-peak [$\Phi(v_1,v_2)$] becomes negative, and the intensities of the two peaks at v_1 and v_2 vary in opposite directions (one increases, the other decreases) under perturbation. On the basis of analysis of the cross-peaks in synchronous and asynchronous maps, we can obtain the specific order of the spectral intensity changes occurring when a sample is subjected to environmental perturbation. According to Noda's rule,[48−50] when $\Phi(v_1,v_2)$ is zero and $\Psi(v_1,v_2)$ is positive (red region), the intensity change of v_1 occurs prior to that of v_2. If $\Psi(v_1,v_2)$ is negative (blue region), the intensity change of v_1 will occur after that of v_2. This rule is reversed, however, when $\Phi(v_1,v_2)$ is zero. On the basis of this unique feature of asynchronous spectra, we obtained additional information concerning the specific interactions in the PVPh-*b*-PDMAEMA copolymer and the PVPh/partially protonated PDMAEMA blends.

Figures 4 and 5 display the synchronous and asynchronous maps of the block copolymers and blend systems in the range 1490−1780 cm^{-1}. Figure 4a (synchronous map) reveals bands at 1730 cm^{-1} for the free C=O groups of PDMAEMA and 1510 or 1612 cm^{-1} for the phenyl−OH bonds of PVPh. Two auto- and cross-peaks at 1730 and 1510 cm^{-1} indicate the specific interactions occurring between these two groups. According to

Table 2. Fraction of Hydrogen-Bonding Groups of PVPh-*b*-PDMAEMA at Room Temperature

block copolymer	H-bonded C=O			free C=O			
	ν (cm^{-1})	$W_{1/2}$	A_f (%)	ν (cm^{-1})	$W_{1/2}$	A_b (%)	f_b (%)
PVPh$_{14}$-*b*- PDMAEMA$_{86}$	1712	27	17	1731	25	83	12
PVPh$_{32}$-*b*- PDMAEMA$_{68}$	1712	28	22	1730	24	78	15.8
PVPh$_{55}$-*b*- PDMAEMA$_{45}$	1711	28	30	1731	25	70	22.2
PVPh$_{70}$-*b*- PDMAEMA$_{30}$	1711	28	40.4	1731	25	59.6	31.1

polymer blend	H-bonded C=O			free C=O			
	ν (cm^{-1})	$W_{1/2}$	A_f (%)	ν (cm^{-1})	$W_{1/2}$	A_b (%)	f_b (%)
PVPh$_{14}$ /PDMAEMA$_{86}$	1708	28	16.3	1730	28	83.7	11.5
PVPh$_{32}$ /PDMAEMA$_{68}$	1709	28	19.4	1730	28	80.6	13.8
PVPh$_{55}$ /PDMAEMA$_{45}$	1709	28	25	1731	27	75	18.2
PVPh$_{70}$ /PDMAEMA$_{30}$	1708	28	30	1730	28	70	22.2

the sign of the cross-peaks at (1730, 1510) cm^{-1} in Figure 4, the intensity of the band at 1510 cm^{-1} increases, while the band at 1730 cm^{-1} decreases (i.e., changes in opposite directions). Obviously, the intensity of the signal for the free C=O groups of PDMAEMA decreased upon increasing the PVPh content because more OH groups were available to interact with them. In contrast, the signs of the weak cross-peaks appearing at (1705, 1510) cm^{-1} in the block copolymer were both positive, implying that increasing the PVPh content induced intensity variations for the two peaks at 1705 and 1510 cm^{-1} in the same direction; i.e., the number of hydrogen-bonded C=O groups increased upon increasing the PVPh content. Note, however, that the intensities of the auto- and cross-peaks at 1510 and 1730 cm^{-1} for the blend system in Figure 4b were relatively weaker than

those for the block copolymer in Figure 4a. This result can be explained in terms of the difference between the interassociation equilibrium constants (K_A), which describe the extent of interassociation of PDMAEMA with PVPh, of the PVPh-*b*-PDMAEMA copolymers and the PVPh/partial protonated PDMAEMA blends. As mentioned above in the discussion of the difference in the degrees of rotation freedom between blend and block copolymer, the polymer chain architecture of a homopolymer is significantly different from that of a block copolymer because of intramolecular screening and functional group accessibility caused by the covalent bond connectivity of the latter. This phenomenon implies that the effective interassociation equilibrium constant of the block copolymer is greater than that of the blend system. As a result of the greater interasso-
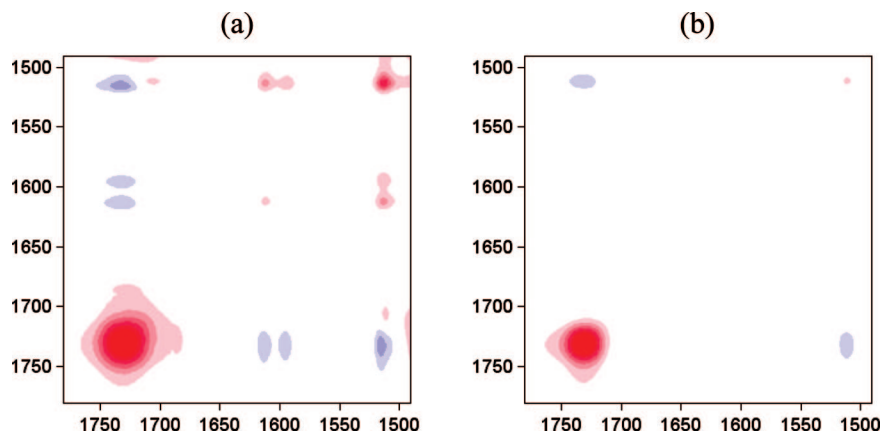
Figure 4. Synchronous 2D correlation map (1490–1780 cm^{-1}) for (a) PVPh-*b*-PDMAEMA diblock copolymers and (b) PVPh/partially protonated PDMAEMA blends.
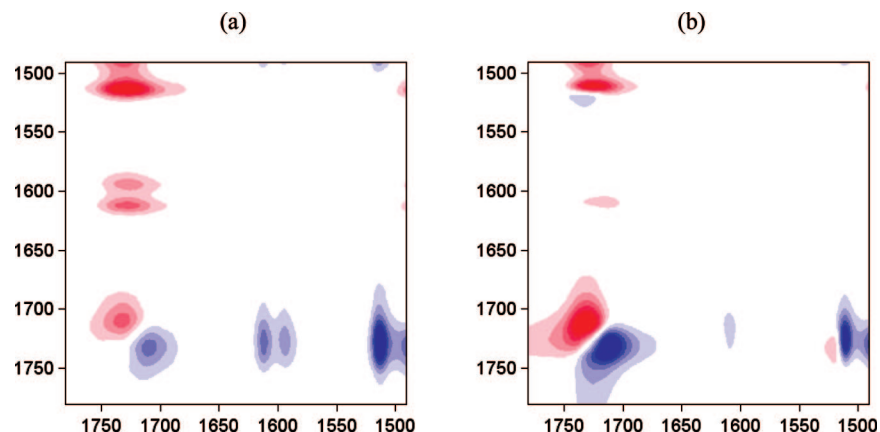
Figure 5. Asynchronous 2D correlation map (1490–1780 cm^{-1}) for (a) PVPh-*b*-PDMAEMA diblock copolymers and (b) PVPh/partially protonated PDMAEMA blends.
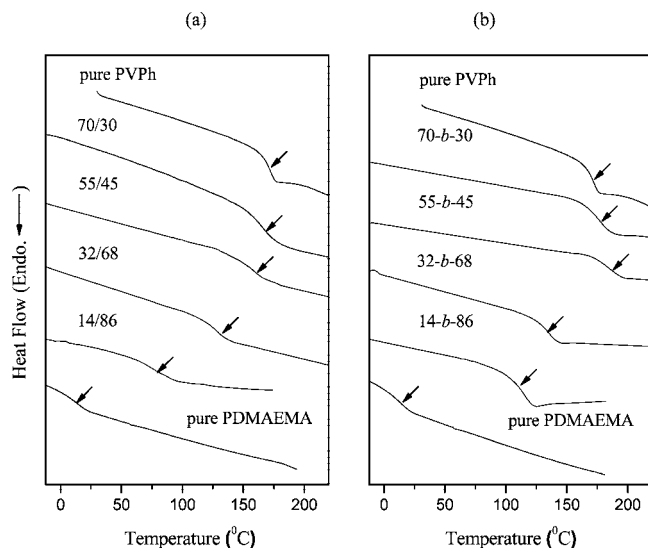
Figure 6. DSC curves of (a) PVPh/partially protonated PDMAEMA blends and (b) PVPh-*b*-PDMAEMA diblock copolymers.

ciation equilibrium constant, the auto- and cross-peaks of the block copolymer are stronger than those of the blend system. This result also infers that the polymer chains in the blends and copolymers display different chain behavior.

The asynchronous 2D-IR correlation spectra in Figure 5 are asymmetric with respect to the diagonal line. The positive cross-peaks at (1730, 1510) cm^{-1} reveal that the out-of-phase spectral changes occur at two wavenumbers.[48] As explained by Noda,[48−50] the cross-peaks of the block copolymer and blend have opposite signs in the synchronous and asynchronous maps, implying that when the content of PVPh is increased, the intensity of the band at 1510 cm^{-1} varies before the band at 1730 cm^{-1} does. This result can be explained in terms of the difference in compatibility between PVPh and PVPh and between PVPh and PDMAEMA. Because self-association OH···OH hydrogen bonding is stronger than interassociation OH···O=C hydrogen bonding, the compatibility between OH groups is higher than that between OH and C=O groups. Therefore, OH groups tend to interact with other OH groups preferentially, rather than with C=O groups, upon increasing the PVPh content. Another reason for the intensity changing in the order OH groups ⟩C=O groups for PVPh-*b*-PDMAEMA is due to the architecture of the polymer chains. Upon increasing the PVPh content, these OH groups are closer to other OH groups in the block copolymer and, thus, make more contacts with neighboring OH groups than with C=O groups. Another positive cross-peak centered at (1730, 1705) cm^{-1} can be identified in Figure 5; it exhibits the same sign in the synchronous maps, implying that the intensity of the peak at 1730 cm^{-1} changes prior to that of the one at 1705 cm^{-1}. Thus, the C=O groups do indeed interact with the OH groups first to form hydrogen-bonded C=O groups. The observed cross-peaks at (1730, 1510) and (1730, 1705) cm^{-1} in the 2D maps provide clear evidence that the sequence changes of these three bands occur in the order 1510 > 1730 > 1705 cm^{-1} (where ">" means "changes prior to").

Thermal Analyses. Generally, only a single glass transition temperature can be observed when the components of blends and block polymers are thermodynamically miscible. Figure 6 presents the DSC thermograms of PVPh-*b*-PDMAEMA block copolymers and blends containing various PVPh contents, revealing that essentially all of the DSC traces possess only a single glass transition temperature, strongly suggesting that these systems are fully miscible and possess a homogeneous amorphous phase. Meanwhile, these single values of T_g were all
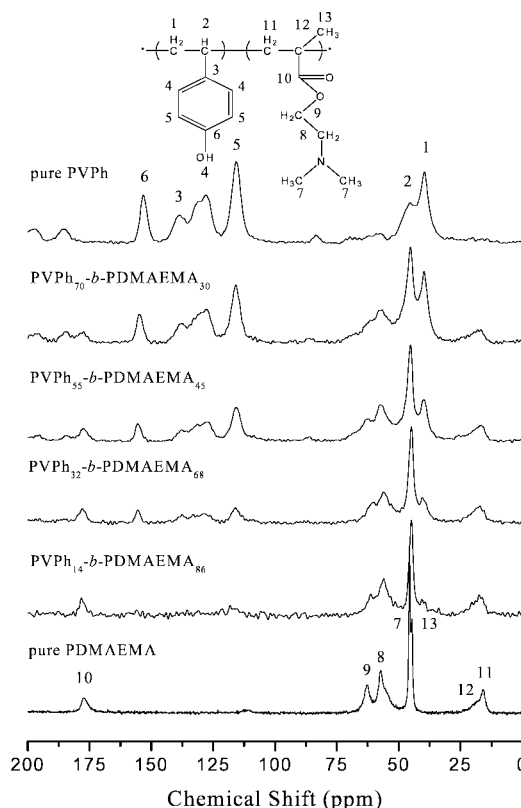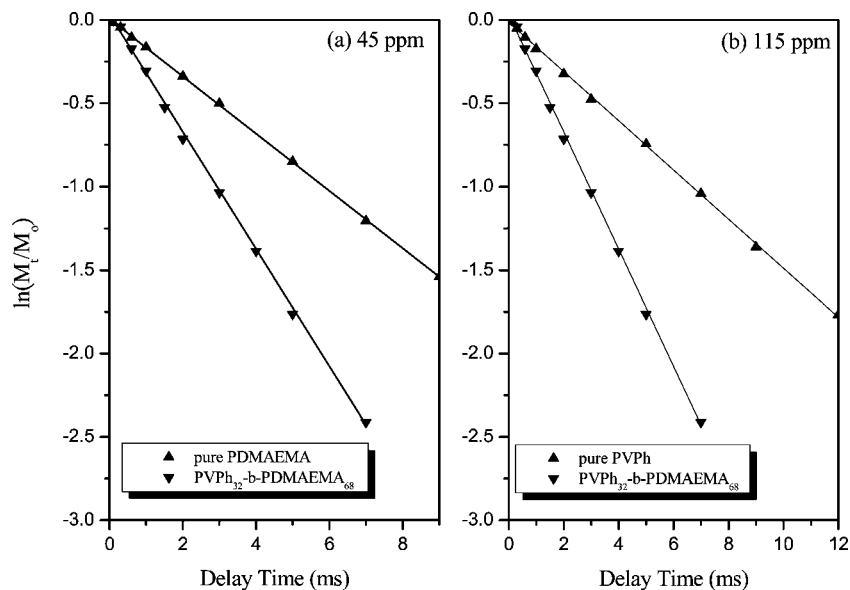

Figure 7. ^{13}C CP/MAS NMR spectra of PVPh-*b*-PDMAEMA diblock copolymers containing various PVPh compositions.

higher than that of the pure PDAMEMA, even when the composition of PVPh in the block copolymer was low. The high positive deviation in the value of T_g of the copolymer indicates that a strong interaction exists between its two blocks. This result is similar to the T_g behavior of the PVPh/partially protonated PDMAEMA miscible blend obtained from a DMSO solution. Over the years, a number of empirical equations have been offered to predict the variations in glass transition temperatures of miscible blends and diblock copolymers as a function of composition. The Kwei equation[51] is usually employed for systems displaying specific interactions:

$$T_g = \frac{W_1 T_{g1} + k W_2 T_{g2}}{W_1 + k W_2} + q W_1 W_2 \qquad (1)$$

where w_1 and w_2 are the weight fractions of the components, T_{g1} and T_{g2} are the corresponding glass transition temperatures, and k and q are fitting constants. The parameter q corresponds to the strength of specific interactions in the system, reflecting a balance between the breaking of the self-association interactions and the forming of the interassociation interactions. Using a nonlinear least-squares "best fit" method, we obtained (Figure S5) values for k and q of 1 and 390, respectively, for the block copolymers and 1 and 240, respectively, for the blends. A greater positive value of q corresponds to stronger interactions between the OH groups of the PVPh segment and the tertiary ammonium groups of the PDMAEMA segment in addition to the self-association of the OH groups of PVPh. The dependence of T_g on the composition not only obeys the thermodynamics of interaction enthalpy but also must take into account the chain conformation entropy of the polymer chain. Additionally, the high positive values of q (390 and 240) obtained for these systems indicate that the interassociation hydrogen-bonding interactions existing between the OH groups of PVPh and the C=O oxygen atoms, nitrogen atoms, and the tertiary ammonium groups of PDMAEMA in the block copolymers were stronger

Figure 8. Logarithmic plots of the intensities of the signals at (a) 45 and (b) 115 ppm with respect to the delay time from the ^{13}C CP/MAS NMR spectra of PVPh-*b*-PDMAEMA diblock copolymers.

Table 3. Relaxation Times, $T_{1\rho}^{H}$, for Blends, Blend Complexes, and Diblock Copolymers at Magnetization Intensities of 45 and 115 ppm

45 ppm		115 ppm	
sample	$T_{1\rho}^{H}$ (ms)	sample	$T_{1\rho}^{H}$ (ms)
pure PDMAEMA	5.82	pure PDMAEMA	
14-*b*-86	3.17	14-*b*-86	2.89
32-*b*-68	2.85	32-*b*-68	3.26
55-*b*-45	4.19	55-*b*-45	3.69
70-*b*-30	4.04	70-*b*-30	3.77
55/45 complex	5.30	55/45 complex	5.60
55/45 blend	5.60	55/45 blend	6.52
pure PVPh		pure PVPh	6.78

than those corresponding interactions in the blends; this finding is similar to those of our previous studies.[20,42,52]

The PVPh$_{55}$-*b*-PDAMEMA$_{45}$ diblock copolymer displays a single glass transition at 184 °C, close to the value of T_g of the PVPh/partially protonated PDMAEMA = 55:45 complex (179 °C) obtained from methanol solution (Table S1). This result can be explained in terms of the polymer chain behavior. Jiang et al.[53,54] reported that an ordinary miscible blend formed an interpolymer complex upon increasing the density of intermolecular hydrogen bonds and that the transition from separated polymer coils to complex aggregates took place in solution where intermolecular hydrogen bonding is strong. They also found that, in the solid state, further strengthening of hydrogen bonding can transform a miscible blend into a complex state. In a previous study,[7] we found that the polymer chain behavior in PVPh-*b*-P4VP diblock copolymers is similar to that in interpolymer complexes because of strong hydrogen bonding between the OH groups of PVPh and the pyridine groups of P4VP. Therefore, we speculate that our PVPh-*b*-PDMAEMA diblock copolymers may display the same polymer chain behavior because of strong interactions between the OH groups of PVPh and the tertiary ammonium groups of PDMAEMA. Thus, we used solid state NMR spectroscopic analyses to determine the spin−lattice relaxation time in the rotating frame and, thereby, investigate the homogeneity of the polymer blends and diblock copolymers.

Solid State NMR Spectroscopic Analyses. Evidence for specific interactions within polymer blends and copolymers can be determined from changes in chemical shifts or line shapes of solid state NMR spectra. Moreover, the molecular mobility
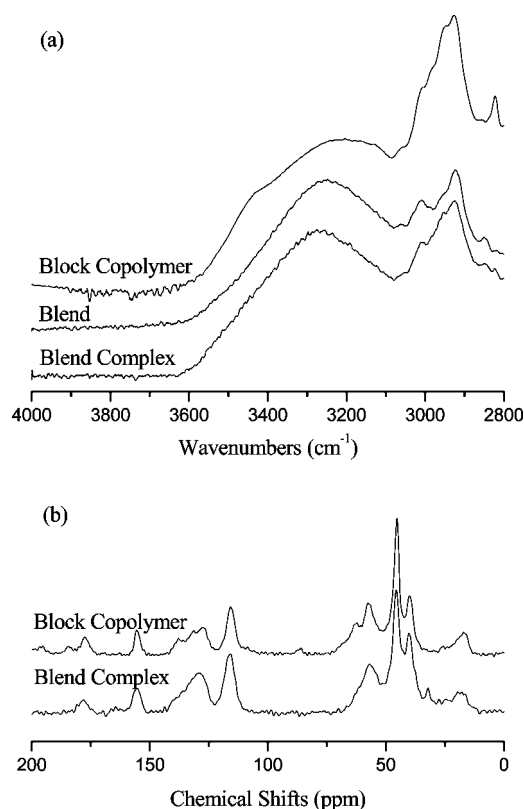
Figure 9. (a) FTIR and (b) ^{13}C solid state NMR spectra of the diblock copolymer, blend complex, and blend having a PVPh:PDMAEMA ratio of 55:45.

of a polymer blend or copolymer can be estimated from the proton spin−lattice relaxation time in the rotating frame ($T_{1\rho}^{H}$), measured using solid state NMR spectroscopy. Figure 7 presents the ^{13}C CP/MAS spectra (with peak assignments) of pure PVPh, pure PDMAEMA, and various PVPh-*b*-PDMAEMA copolymers. Table S2 summarizes the chemical shifts observed in the ^{13}C CP/MAS spectra of PVPh-*b*-PDMAEMA copolymers. The signal of the phenolic carbon atom of PVPh at 153.3 ppm underwent a gradual downfield shift upon increasing the PVPh content. A shift of ca. 3 ppm occurred for the diblock copolymer containing 84 mol % PDMAEMA, indicating that specific
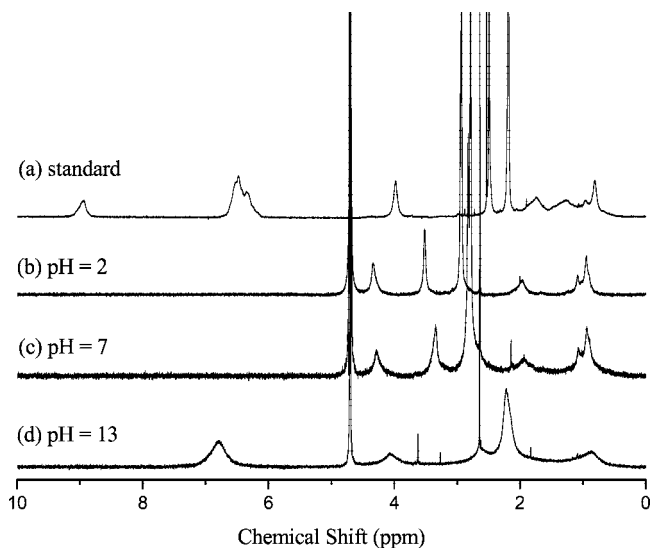
Figure 10. ¹H NMR spectra of the PVPh$_{32}$-*b*-PDMAEMA$_{68}$ diblock copolymer in (a) DMSO-d_6, (b) D$_2$O at pH 2, (c) D$_2$O at pH 7, and (d) D$_2$O at pH 13.

interactions were indeed present between the PVPh and PDMAEMA blocks, consistent with the results of our earlier FTIR spectroscopic analyses.

Solid state NMR spectroscopy can be used to understand the phase behavior and miscibility of diblock copolymers and blends. A single value of T_g determined through DSC analysis reveals that the mixing of two blending components occurs on a scale of ca. 20−40 nm.[4] Dimensions of mixing less than 20 nm can be obtained through measurement of the spin−lattice relaxation time in the rotating frame ($T_{1\rho}^H$).[4] We estimated the values of $T_{1\rho}^H$ of the diblock copolymers and blend complexes through delayed-contact ¹³C CP/MAS experiments, using the equation

$$M_\tau = M_0 \exp[-\tau/T_{1\rho}(H)] \qquad (2)$$

where τ is the spin-lock time used in the experiment and M_0 and M_τ are the intensities of the peaks initially and at time τ, respectively. Figures 8a,b display typical plots of $\ln(M_\tau/M_0)$ vs τ for the PDMAEMA resonance at 45 ppm and the PVPh resonance at 115 ppm of the diblock copolymer. The experimental data obtained are in good agreement with eq 2. We determined the value of $T_{1\rho}^H$ from the slope of the fitting line. All of the copolymers, blends, and blend complexes exhibited only a single composition-dependent value of $T_{1\rho}^H$; Table 3 reveals the high miscibility and dynamic homogeneity of both the PVPh and PDAMEMA phases. These results are also consistent with our earlier DSC analyses. The single values of $T_{1\rho}^H$ for the PVPh-*b*-PDMAEMA and blend complexes are lower than that for the corresponding PVPh/partially protonated PDMAEMA blend. This observation suggests that the domain size of the diblock copolymer is smaller relative to that of the corresponding polymer blend; i.e., the degree of homogeneity of the diblock copolymer is relatively higher than that of the blend. The shorter $T_{1\rho}^H$ relaxation time of the block copolymer suggests a more rigid nature of the polymer chain and a higher value of T_g. A similar trend has been observed previously: the values of $T_{1\rho}^H$ of polymer blends of poly(acrylic acid) (PAA)/ polyvinylpyrrolidone (PVP) are greater than those of blend complexes of PAA/PVP.[55] We have reported previously that the polymer chain behavior of the strongly hydrogen-bonded PVPh-*b*-P4VP diblock copolymer occurs in the form of complex aggregates, similar to the interpolymer PVPh/P4VP complex obtained from methanol solution.[7] Therefore, we conclude that the different behavior in the values of T_g between PVPh-*b*-

PDAMEMA diblock copolymers and their corresponding blends resulted from their different chain conformations. To confirm this behavior, we compared the FTIR spectra and ¹³C solid state NMR spectra of the PVPh-*b*-PDMAEMA copolymers with those of their corresponding blends and blend complexes. Figure 9 presents the FTIR spectra (OH stretching region) and ¹³C solid state NMR spectra of the blend, blend complex, and diblock copolymer having a PVPh-to-PDMAEMA ratio of 55:45. We observe that the signal of the phenolic carbon atom (C-6) at 153 ppm for both the diblock copolymer and blend complex shifted downfield by the same amount. Moreover, the OH stretching signal for the specific interaction was also shifted by the same amount in the FTIR spectra of the blend, blend complex, and block copolymer, indicating that the specific interaction had identical strength in all systems. We observed, however, that the relative intensity ratio of the OH···OH (3350 cm⁻¹) and OH···tertiary ammonium (3220 cm⁻¹) hydrogen-bonded signals was greater for the copolymer. As a result, we speculate that intrachain contacts play an important role in the block copolymer system. On the basis of our DSC, solid state NMR spectroscopic, and FTIR spectroscopic analyses, we deduce that the polymer chain behavior of the PVPh-*b*-PDMAEMA copolymers occurs through strong specific interactions in the form of a complex, similar to that in the interpolymer complex formed from PVPh and the partially protonated PDMAEMA obtained from methanol solution. The polymer chains of a miscible polymer blend are well separated in a highly polar solvent (e.g., DMF or DMSO) prior to solvent evaporation when, for example, the interassociation hydrogen bonding between PVPh/DMSO is stronger than that in the PVPh/partial protonated PDMAEMA blend. Nevertheless, copolymer complex aggregation can occur because of the higher strength of intrachain interactions in diblock copolymer chains. Two possible mechanisms may be involved in the formation of interpolymer complexes: (i) two individual diblock copolymer chains interact through interchain hydrogen bonding or (ii) an intrapolymer complex forms through folding of the same diblock copolymer chain through intrachain hydrogen bonding. For a polymer blend, the interchain interaction is the only route available to form a complex. This result is consistent with our FTIR spectral observation that the relative intensities of the signals for the OH···OH, OH···O=C, OH···N, and OH···tertiary ammonium interactions in the blend complex system were low, indicating that most interactions resulted from interchain contact. As a result, both the inter- and intrapolymer complexes in the diblock copolymer have smaller domain sizes than the relatively more separated coils in the miscible blend, consistent with the values of $T_{1\rho}^H$. Again, we employed 2D-IR correlation spectroscopy to confirm the existence of intrachain interactions for PVPh-*b*-PDMAEMA. Figure S6a presents the synchronous 2D correlation maps in the range from 2700 to 3800 cm⁻¹. Clearly, positive cross-peaks exist in this range from 3200 to 3500 cm⁻¹, corresponding to the OH stretching signals of the PVPh block, implying that the hydrogen-bonding interactions did indeed occur between the OH groups. In contrast, the corresponding asynchronous 2D correlation map for PVPh-*b*-PDMAEMA (Figure S6b) does not reveal any auto- or cross-peaks within the same wavenumber range, implying that the OH groups of the PVPh block undergo intramolecular hydrogen-bonding interactions.

pH-Induced Micellization of PVPh-*block*-PDMAEMA Copolymers. PDMAEMA is a weak polybase that is soluble in neutral and acidic media because of its protonated tertiary amino groups; PVPh is soluble in basic media as a result of the ionization of its OH groups. Therefore, we anticipated that the PVPh-*b*-PDMAEMA diblock copolymer might display pH-reversible micellization behavior, forming micelles with hydro-
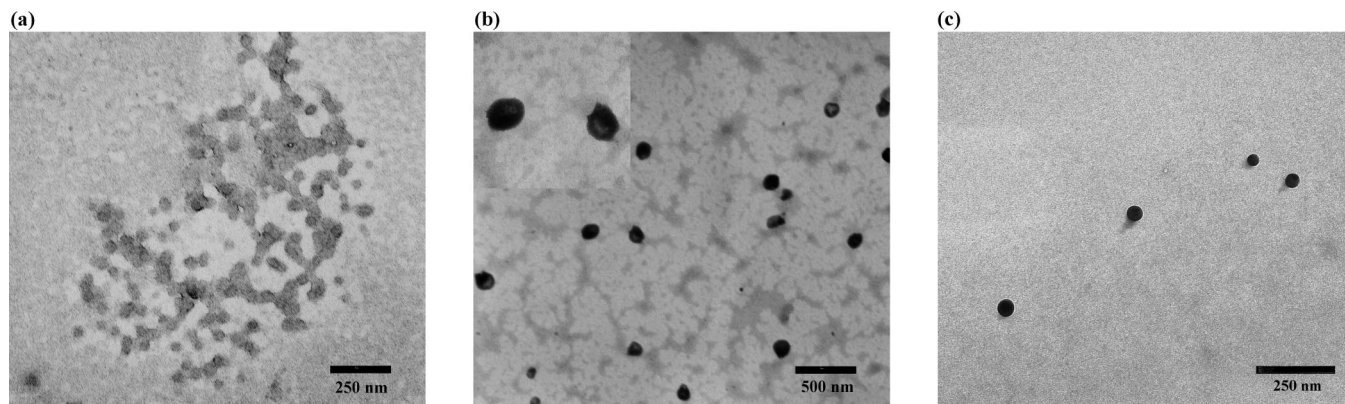
Figure 11. TEM images of the morphologies of the PVPh$_{32}$-*b*-PDMAEMA$_{68}$ diblock copolymer prepared in aqueous media at (a) pH 2, (b) pH 7, and (c) pH 13.
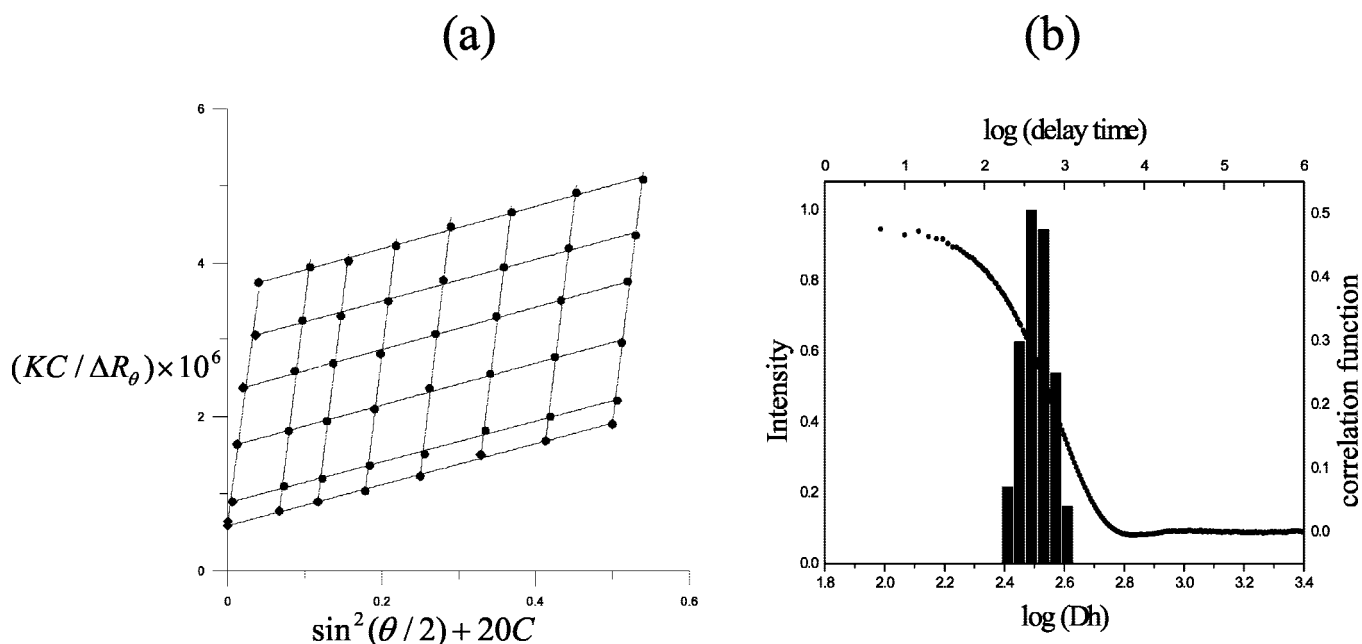

Figure 12. (a)Zimm plot analysis and (b) the hydrodynamic radius distribution of the PVPh$_{32}$-*b*-PDMAEMA$_{68}$ block copolymer in aqueous media at pH 7.

phobic PVPh cores and hydrophilic PDMAEMA shells at low pH and hydrophilic PDMAEMA cores and hydrophobic PVPh shells at high pH. To confirm the pH-sensitive behavior of the PVPh-*b*-PDMAEMA diblock copolymer, we analyzed NMR spectra and TEM images of PVPh$_{32}$-*b*-PDMAEMA$_{68}$ at various values of pH.

Figure 10 displays the ^{1}H NMR spectra of PVPh$_{32}$-*b*-PDMAEMA$_{68}$ in D$_2$O under acidic (pH 2), neutral (pH 7), and basic (pH 13) conditions, with reference to the spectrum of the copolymer in DMSO-d_6 as a standard. The signals due to the aromatic protons of PVPh at 6.1−6.9 ppm disappeared at both neutral and acidic pH, while the signals due to the ethyl protons of PDMAEMA at 4.2−4.4 ppm remained prominent. In contrast, the signal due to the aromatic protons of PVPh at 6.1−6.9 ppm was present at pH 13, whereas the signal due to the ethyl protons of PDMAEMA at 4.2−4.4 ppm was suppressed and broadened, indicating the lower mobility and decreasing solvation of these blocks. These NMR spectral data revealed subtle variations in the hydrophilic/hydrophobic balance of the diblock copolymer, providing a unique opportunity to prepare either PVPh−core micelles or PDMAEMA−core micelles from the same copolymer merely by changing the pH of the solution; i.e., pH-induced micellar self-assembly of PVPh-*b*-PDMAEA.

Figure 11 displays TEM images of the morphologies formed from PVPh$_{32}$-*b*-PDMAEMA$_{68}$ at various values of pH. Nanospherical micelles of PVPh$_{32}$-*b*-PDMAEMA$_{68}$ formed at pH 2 (Figure 11a). To our surprise, these spherical micelles transformed into vesicles when we increased the pH to 7 (Figure 11b). Meanwhile, we have been carried out the dynamic light scattering and static light scattering measurements for confirming the structure of the PVPh$_{32}$-*b*-PDMAEMA$_{68}$ block copolymer in aqueous media at pH 7. The ratio R_g/R_h provides an indication of the shape of the scattering particle, for example, the ratio of hard sphere is 0.775, the ratio of random coil is near 1.5, and the ratio of vesicle is ~1.[59] Figure 12 presents the static light scattering and dynamic light scattering analyses of the PVPh$_{32}$-*b*-PDMAEMA$_{68}$ block copolymer in aqueous media at pH 7. The values of R_g and R_h which are 186.46 and 175.25 nm, respectively, can be obtained from the DLS and SLS analyses of the PVPh$_{32}$-*b*-PDMAEMA$_{68}$ block copolymer in aqueous media at pH 7. Therefore, the ratio R_g/R_h which is 1.06 can be obtained. On the basis of the value of R_g/R_h which is ~1, we can further confirm that the structure of the aggregates of the PVPh$_{32}$-*b*-PDMAEMA$_{68}$ block copolymer in aqueous media at pH 7 is vesicle. When we increased the pH further (to pH 13), these aggregates return to the form of nanospherical micelles
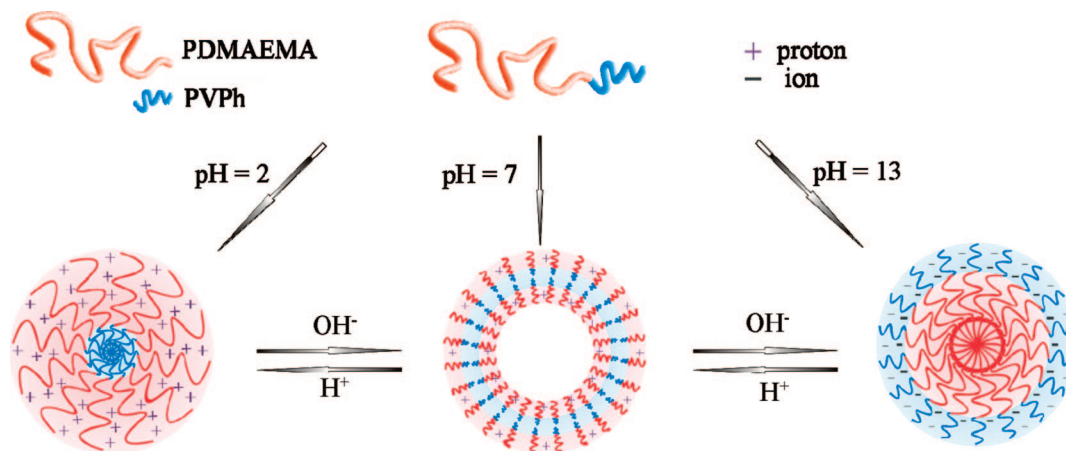
Figure 13. Proposed pH-dependent microstructural transformations of the PVPh$_{32}$-*b*-PDMAEMA$_{68}$ diblock copolymer.

(Figure 11c). Several factors influence the morphologies of block copolymer aggregates in a solution;[56,57] the free energies of aggregation are affected by the intercoronal chain interaction, the core−coronal interfacial energy, and the degree of core−chain stretching. At pH 2, the spherical micelles formed as result of the hydrophobic interactions of the uncharged PVPh blocks in water. Only small fraction of the protonated PDAMEAM interacted with the OH groups of PVPh, while the remaining protonated PDMAEMA units formed the corona of the micelle, thereby stabilizing its structure. Thus, at low pH, we suspect that each spherical micelle comprised (i) a core of hydrophobic PVPh blocks and some PVPh/protonated PDMAEMA complexes and (ii) a cationic PDMAEMA corona. Upon increasing the pH to 7, the PDMAEMA blocks began to lose some of their cationic character as a result of deprotonation of the ammonium units, resulting in a decrease in the strength of the electrostatic repulsive interactions among the corona chains. Consequently, the size of the aggregates increased to reduce the interfacial energy between the core and the solvent. The degree of stretching of the PVPh chains increased because the interactions between the PVPh and PDMAEMA segments became weaker, indicating that the entropic penalty increased. To reduce the total free energy in the system, the aggregates transformed their morphology from spherical micelles to vesicles.[58] At pH 13, the tertiary amino groups of PDMAEMA were almost completely deprotonated and, thus, these blocks became particularly hydrophobic;[32] in contrast, the PVPh blocks were completely ionized in their anionic form. Nevertheless, a few signals at 4.2−4.4 ppm due to the ethyl protons of PDMAEMA were still evident in the NMR spectrum, indicating that the PDMAEMA blocks remained partially solvated, i.e., the micellar core retained some degree of hydration; similar observations have been reported by Lowe et al. for the micellization of PDMAEMA-*b*-PMAA diblock copolymers.[31] Therefore, at high pH, the spherical micelles comprised PDMAEMA hydrated cores and PVPh anionic coronas.

Figure 13 displays our proposed microstructures for the PVPh$_{32}$-*b*-PDMAEMA$_{68}$ diblock copolymer at various values of pH. At pH 2, compact spherical micelles formed from the hydrophobic association of the PVPh segments and a few PVPh/protonated PDMAEMA complexes, driven by entropic considerations—i.e., a gain in entropy occurred when water molecules were released from the disrupted solvent cage surrounding the hydrophobic PVPh segments. At pH 7, the electrostatic repulsive forces among protonated PDMAEMA segments weakened and the stretching of PVPh segments increased. As a result, the morphology of the diblock copolymer transformed from spherical micelles to vesicles to reduce the free energy of the system. At pH 13, the aggregates change shape from vesicles to spherical

micelles comprising ionized-PVPh−coronas and deprotonated-PDMAEMA−hydrated cores—i.e., a phase inversion of the structure of the micelles formed at pH 2.

Conclusions

We have synthesized novel pH-sensitive PVPh-*b*-PDMAE-MA diblock copolymers through anionic polymerization. FTIR and solid state NMR spectroscopic analyses provided evidence for strong interactions existing between the OH groups of PVPh and the tertiary ammonium groups of PDMAEMA. From DSC analyses, we observed that the glass transition temperatures of the diblock copolymers increased significantly as a result of strong interactions between the OH groups of PVPh and the tertiary ammonium groups of PDMAEMA. ^{1}H NMR spectroscopic and TEM analyses revealed the pH-sensitive self-assembly behavior of PVPh-*b*-PDMAEMA diblock copolymer in aqueous media. At pH 2, spherical micelles formed comprising a neutral PVPh block surrounded by a protonated-PD-MAEMA block corona. At pH 7, the diblock copolymer's morphology transformed into vesicles to reduce the free energy of the system. At pH 13, these aggregates changed from vesicles to spherical micelles comprising ionized-PVPh coronas and hydrated deprotonated-PDMAEMA cores−i.e., phase-inversed micelles relative to those formed at pH 2.

Supporting Information Available: Full data (tables and figures) of diblock copolymers characterization such as IR and DSC. This material is available free of charge via the Internet at http://pubs.acs.org.

References and Notes

(1) Utracki, L. A. *Polymer Alloys and Blends: Thermodynamics and Rheology*; Carl Hanser Verlag: Munich, 1989.
(2) Coleman, M. M.; Graf, J. F.; Painter, P. C. *Specific Interactions and the Miscibility of Polymer Blends*; Technomic Publishing: Lancaster, PA, 1991.
(3) Coleman, M. M.; Painter, P. C. *Prog. Polym. Sci.* **1995**, *20*, 1.
(4) Kuo, S. W.; Chang, F. C. *Macromolecules* **2001**, *34*, 4089.
(5) Kuo, S. W.; Chang, F. C. *Macromolecules* **2001**, *34*, 5224.
(6) He, Y.; Zhu, B.; Inoue, Y. *Prog. Polym. Sci.* **2004**, *29*, 1021.
(7) Serman, C. J.; Painter, P. C.; Coleman, M. M. *Polymer* **1991**, *32*, 1049.
(8) Zhang, X.; Takegoshi, K.; Hikichi, K. *Macromolecules* **1991**, *24*, 5756.
(9) Li, D.; Brisson, J. *Macromolecules* **1996**, *29*, 868.
(10) Dong, J.; Ozaki, Y. *Macromolecules* **1997**, *30*, 286.
(11) Kuo, S. W.; Liu, W. P.; Chang, F. C. *Macromolecules* **2003**, *36*, 5165.

(12) Kuo, S. W.; Liu, W. P.; Chang, F. C. *Macromol. Chem. Phys.* **2005**, *206*, 2307.

(13) Huang, X. D.; Goh, S. H.; Lee, S. Y.; Zhao, Z. D.; Wong, M. W.; Huan, C. H. A. *Macromolecules* **1999**, *32*, 4327.

(14) Kuo, S. W.; Tung, P. H.; Lai, C. L.; Jeong, K. U.; Chang, F. C. *Macromol. Rapid Commun.* **2008**, *29*, 229.

(15) Wang, L. F.; Pearce, E. M.; Kwei, T. K. *J. Polym. Sci., Polym. Phys. Ed.* **1991**, *29*, 619.

(16) Dai, J.; Goh, S. H.; Lee, S. Y.; Siow, K. S. *Polym. J.* **1994**, *26*, 905.

(17) Luo, X. F.; Goh, S. H.; Lee, S. Y. *Macromolecules* **1997**, *30*, 4934.

(18) Liu, Y.; Goh, S. H.; Lee, S. Y.; Huan, C. H. A. *Macromolecules* **1999**, *32*, 1967.

(19) Zhong, Z.; Guo, Q. *Polym. Int.* **1996**, *41*, 315.

(20) Kuo, S. W.; Tung, P. H.; Chang, F. C. *Macromolecules* **2006**, *39*, 9388.

(21) Butun, V.; Billingham, N. C.; Armes, S. P. *J. Am. Chem. Soc.* **1998**, *120*, 11818.

(22) Butun, V.; Billingham, N. C.; Armes, S. P.; et al. *Macromolecules* **2001**, *34*, 1503.

(23) Liu, S. Y.; Billingham, N. C.; Armes, S. P. *Angew. Chem., Int. Ed.* **2001**, *40*, 2328.

(24) Bories-Azeau, X.; Armes, S. P.; Van den Haak, H. J. W. *Macromolecules* **2004**, *37*, 2348.

(25) Liu, S.; Armes, S. P. *Langmuir* **2003**, *19*, 4432.

(26) Mountrichas, G.; Pispas, S. *Macromolecules* **2006**, *39*, 4767.

(27) Butun, V.; Billingham, N. C.; Armes, S. P. *J. Am. Chem. Soc.* **1998**, *120*, 12135.

(28) Dou, H. J.; Jiang, M. *Angew. Chem., Int. Ed.* **2003**, *42*, 1516.

(29) Butun, V.; Top, R. B.; Ufuklar, S. *Macromolecules* **2006**, *39*, 1216.

(30) Wan, S.; Jiang, M.; Zhang, G. *Macromolecules* **2007**, *40*, 5552.

(31) Lowe, A. B.; Billingham, N. C.; Armes, S. P. *Macromolecules* **1998**, *31*, 5991.

(32) Gohy, J. F.; Creutz, S.; Garcia, M.; Mahltig, B.; Stamm, M.; Jerome, R. *Macromolecules* **2001**, *33*, 6378.

(33) Varshney, S. K.; Zhong, X. F.; Eisenberg, A. *Macromolecules* **1993**, *26*, 701.

(34) Quirk, R. P.; Corona-Galvan, S. *Macromolecules* **2001**, *34*, 1192.

(35) Biggs, S.; Vincent, B. *Colloid Polym. Sci.* **1992**, *270*, 505.

(36) Hubert, P.; Soum, A.; Fontanille, M. *Macromol. Chem. Phys.* **1995**, *196*, 1023.

(37) Quirk, R. P.; Lee, Y. *J. Polym. Sci., Part A: Polym. Chem.* **2000**, *38*, 145.

(38) Jiang, X.; Tanaka, K.; Takahara, A.; Kajiyama, T. *Polymer* **1998**, *39*, 2615.

(39) Pullman, A.; Berthier, G.; Savinelli, R. *J. Am. Chem. Soc.* **1998**, *120*, 8553.

(40) Moskala, E. J.; Varnell, D. F.; Coleman, M. M. *Polymer* **1985**, *26*, 228.

(41) Moritani, T.; Fujiwara, Y. *Macromolecules* **1977**, *10*, 532.

(42) Lin, C. L.; Chen, W. C.; Liao, C. S.; Su, Y. C.; Huang, C. F.; Kuo, S. W.; Chang, F. C. *Macromolecules* **2005**, *38*, 6435.

(43) Painter, P. C.; Veytsman, B.; Kumar, S.; Shenoy, S.; Graf, J. F.; Xu, Y.; Coleman, M. M. *Macromolecules* **1997**, *30*, 932.

(44) Coleman, M. M.; Pehlert, G. J.; Painter, P. C. *Macromolecules* **1996**, *29*, 6820.

(45) Pehlert, G. J.; Painter, P. C.; Veytsman, B.; Coleman, M. M. *Macromolecules* **1997**, *30*, 3671.

(46) Pehlert, G. J.; Painter, P. C.; Coleman, M. M. *Macromolecules* **1998**, *31*, 8423.

(47) Coleman, M. M.; Guigley, K. S.; Painter, P. C. *Macromol. Chem. Phys.* **1999**, *200*, 1167.

(48) Noda, I. *Appl. Spectrosc.* **1993**, *47*, 1329.

(49) Noda, I. *Appl. Spectrosc.* **2000**, *54*, 994.

(50) Noda, I.; Story, G. M.; Marcott, C. *Vib. Spectrosc.* **1999**, *19*, 461.

(51) Kwei, T. K. *J. Polym. Sci., Polym. Lett. Ed.* **1984**, *22*, 307.

(52) Kuo, S. W.; Huang, C. F.; Tung, P. H.; Huang, W. J.; Huang, J. M.; Chang, F. C. *Polymer* **2005**, *46*, 9348.

(53) Jiang, M.; Li, M.; Xiang, M.; Zhou, H. *Adv. Polym. Sci.* **1999**, *146*, 121.

(54) Wang, M.; Jiang, M.; Ning, F. L.; Chen, D. Y.; Liu, S. Y.; Duan, H. W. *Macromolecules* **2002**, *35*, 5980.

(55) Lau, C.; Mi, Y. *Polymer* **2002**, *43*, 823.

(56) Zhang, L.; Eisenberg, A. *Polym. Adv. Technol.* **1998**, *9*, 677.

(57) Zhang, L.; Eisenberg, A. *J. Am. Chem. Soc.* **1996**, *118*, 3168.

(58) Zhang, L.; Eisenberg, A. *Macromolecules* **1996**, *29*, 8805.

(59) Anders, H.; Mats, J.; Eva, M. *Adv. Polym. Sci.* **1999**, *143*, 113.